Available online at BCREC website: https://bcrec.id

Bulletin of Chemical Reaction Engineering & Catalysis, 15 (1) 2020, 104-111

Research Article

Hydrazine and Urea Fueled-Solution Combustion Method for Bi_2O_3 Synthesis: Characterization of Physicochemical Properties and Photocatalytic Activity

Yayuk Astuti[1,*], Prisca Putri Elesta[1], Didik Setyo Widodo[1], Hendri Widiyandari[2], Ratna Balgis[3]

[1]Chemistry Department, Faculty of Sciences and Mathematics, Diponegoro University
Jl. Prof. Soedarto, Kampus Undip Tembalang, Semarang, 50275, Indonesia.
[2]Department of Physics, Faculty of Mathematics and Natural Sciences, University of Sebelas Maret
Jl. Ir Sutami No. 36A, Jebres, Surakarta, 57126, Indonesia.
[3]Department of Chemical Engineering, Faculty of Engineering, Hiroshima University
141 Kagamiyama, Higashi-Hiroshima City Hiroshima, 7398527, Japan.

Received: 24th July 2019; Revised: 18th October 2019; Accepted: 19th October 2019;
Available online: 28th February 2020; Published regularly: April 2020

Abstract

Bismuth oxide synthesis using solution combustion method fuelled by hydrazine and urea has been conducted. This study aims to examine the effect of the applied fuels, urea and hydrazine, on product characteristics and photocatalytic activity in degrading rhodamine B dye. Bismuth oxide synthesis was initiated by dissolving bismuth nitrate pentahydrate ($Bi(NO_3)_3.5H_2O$) in a nitric acid solvent. Fuel was added and then stirred. The solution formed was heated at 300 °C for 8 hours. The product obtained was then calcined at 700 °C for 4 hours. Bismuth oxide synthesized with urea (BO1) and hydrazine (BO2) as fuels both obtained form of yellow powder. The formation of bismuth oxide is indicated by the vibrations of the Bi–O–Bi and Bi–O groups and the crystal structure of α-Bi_2O_3 in both products. Photocatalytic activity test showed that BO1 has a photocatalyst activity in degrading rhodamine B higher than that of BO2 with constant values of 3.83×10^{-5} s^{-1} and 3.43×10^{-5} s^{-1}, respectively. The high photocatalytic activity can be examined through several factors, such as: band gap values, crystal structure, morphology, and surface area, acquired as a result of the use of different fuels in the synthesis process.

Keywords: Bismuth Oxide; Solution Combustion; Photocatalysis; Rhodamine B; Fuels

How to Cite: Astuti, Y., Elesta, P.P., Widodo, D.S., Widiyandari, H., Balgis, R. (2020). Hydrazine and Urea Fueled-Solution Combustion Method for Bi_2O_3 Synthesis: Characterization of Physicochemical Properties and Photocatalytic Activity. *Bulletin of Chemical Reaction Engineering & Catalysis*, 15(1), 104-111 (doi:10.9767/bcrec.15.1.5483.104-111)

Permalink/DOI: https://doi.org/10.9767/bcrec.15.1.5483.104-111

1. Introduction

Bismuth oxide semiconductor has received increasing attention as a photocatalyst in degrading organic pollutants under the influence of UV-A rays. Bismuth oxide has six polymorphs, that are α-Bi_2O_3, β-Bi_2O_3, γ-Bi_2O_3, δ-Bi_2O_3, ε-Bi_2O_3 and ω-Bi_2O_3 which are different in crystal structure and thermal stability [1]. Bismuth oxide has a variety of desirable characteristics including high band gap values (2.3-3.3 eV) [2], high index of refraction (nδBi_2O_3 = 1.9-2.5) [3,4], good photocunductivity and photolu-

* Corresponding Author.
E-mail: yayuk.astuti@live.undip.ac.id (Y. Astuti);
Telp: (+62 24) 7474754, Fax: (+62 24) 7648069

minescence properties [5]. Bismuth oxide has wide forms of use, such as: in solid oxide fuel cells [6,7], gas sensors [8], high temperature superconducting materials [9], functional ceramics [10], and photocatalyst [11-13]. With rapidly increasing research on bismuth oxide, more methods of Bi_2O_3 synthesis have now been discovered. These methods include deposition [11], sol-gel [14], hydrothermal [15], solution combustion [16-18], magnetron sputtering deposition [19], and low-temperature electrodeposition [20]. In this study, solution combustion method (SC) was used in consideration of its time and energy savings and simple production of the desired material. The exothermicity of the chemical reactions in SC synthesis is used to form oxides from the precursor mixture. After the reaction mixture is heated, the heat produced during the reaction is used by the mixture to form the desired product [21].

Various parameters must be considered in the process of synthesis using SC method. The fuel/oxidant ratio, type of fuel, and temperature characteristics are some of the most important. The selection of suitable fuel is a critical parameter because it influences the modification of mechanisms and kinetics of combustion and provides the possibility to control product characteristics. Each fuel acts differently and thus its effects on the nature of the final product must be analysed [22].

Study of effects on product in regards to specific fuel used in the synthesis of a metal oxide through solution combustion method have previously been carried out such as in the synthesis of TiO_2 [23] and NiO [24]. Rasouli *et al.* [23] reported that the synthesis of nanocrystalline TiO_2 achieved the largest crystalline size with citric acid as fuel followed by urea and glycine. The results of analysis of specific surface area with SAA for TiO_2 sample obtained from the use of glycine have the largest surface area, followed by urea and citric acid. Furthermore, Raveendra *et al.* [24] reported that from the results of SEM analysis, the morphology of NiO synthesized with urea was spherical and uniformly distributed, whereas the morphology of NiO synthesized with glycine was more porous. The crystal size and surface area of the synthesized products are also influenced by fuel variations.

Researches on synthesis of TiO_2 and NiO by solution combustion method using urea and glycine as fuels were conducted; however, synthesis of bismuth oxide using the solution combustion method with fuel urea and hydrazine has never been undertaken previously. Astuti *et al.* [17] and La *et al.* [18] have synthesized it but the fuel used was different, that was only citric acid. Therefore, it is important to study the effect of fuels, especially hydrazine and urea on the characteristics of the obtained products; these characteristics are important to determine the potential application of bismuth oxide primarily as photocatalysts. This research aims to investigate the influence of fuels especially hydrazine and urea on bismuth oxide characteristics and photocatalytic activity in degrading rhodamine B dye. The choice of fuel variations is based on the differences in the chemical structure and strength of electron donor groups that are related to the reactivity of each fuel and the effects on the final results of the synthesis material. Hydrazine and urea both have two $–NH_2$ groups that act as electron donors to the nitrate group of bismuth nitrate pentahydrate. The reactivity of the fuel in relation to the bismuth nitrate pentahydrate affects the energy released in the exothermic reaction of the combustion solution. The difference in the reactivity of the two fuels will affect the characteristics of the final products. This investigation is expected to give recommendation on the use of proper fuel in synthesis of bismuth oxide using solution combustion method so that obtained product (bismuth oxide) has high photocatalytic activity and also to give science contribution.

2. Materials and Methods

2.1 Materials

The materials used in this study include bismuth nitrate pentahydrate, rhodamine B (purchased from Sigma Aldrich), nitric acid, urea, hydrazine (bought from Merck) and distilled water. All the chemicals were of analytical grade.

2.2 Bismuth Oxide Synthesis

As much as 1.21 gram of bismuth nitrate pentahydrate was dissolved in 10 mL 0.04 M nitric acid. Then 0.060 gram of urea was added into the mixture as fuel. The mixture solution was then stirred at a speed of 667 rpm for 5 minutes using a magnetic strirer (Cimarec SP131320-33Q). The solution was then heated for 8 hours at 300 ^oC on a hot plate (Cimarec SP131320-33Q). Then the product formed was calcined for 4 hours using a furnace (Eurotherm 2116) at a temperature of 700 ^oC. The synthesis of bismuth oxide with hydrazine as fuel underwent the same procedure however bismuth nitrate pentahydrate and hydrazine

used were 3.63 gram and 0.064 gram, respectively. Results after calcination were then denoted by BO1 and BO2 for the use of urea and hydrazine as fuels, respectively.

2.3 Product Characterization

Characterisations were conducted through FTIR, XRD, SEM, SAA, and DR-UV. The instrument utilized to record FTIR spectra was FTIR Prestige 21 (Shimadzu) with wavenumber of 400-4000 cm^{-1}. The diffractograms were recorded using the XRD instrument (Shimadzu 7000) with Cu-Kα as the radiation source, 30 kV voltage, 30 mA electricity, X-ray radiation wave of 1.54178 Å, and 2θ ranging from 10° to 90°. In order to identify the crystal structure of products, the diffractograms were compared with joint committee on powder diffraction standard (JCPDS) database. Furthermore, SEM images and surface area were obtained using JEOL-JSM-6510LV microscope and Quantachrome v.11.0, respectively. Meanwhile, band gap energy was determined using the DR-UV instrument (UV 1700 Pharmaspec).

2.4 Photocatalytic Activity on Rhodamin B Degradation

Photocatalytic activity test of both BO1 and BO2 products was undertaken in a photocatalytic reactor with and without radiation light. To test photocatalytic activity under UV A, 0.1 g of product was added to 50 mL 5 ppm Rhodamine B. The mixture was stirred at a speed of 667 rpm with varying irradiation time of 1, 2, 3 and 4 hours. Meanwhile, a photocatalytic activity test without light was carried out using the same procedure but only for 2 hours. The photocatalysis solution was then centrifuged to separate the Rhodamin B solution from the bismuth oxide photocatalyst. The resulting supernatant was then analyzed using a UV-Vis spectrophotomater at optimum wavelength (λ_{max}). The optimum wavelength was determined by analyzing 5 ppm of Rh B dye solution without treatment using a UV-Vis spectrophotomater in the wavelength range of 400-800 cm^{-1} and the resulting value λ_{max} was 553 nm. The concentration of dyes from photocatalysis was determined by entering the absorbance value into a linier equation of standard curve.

In addition, degradation percentage of dye after the photocatalytic process with time variations according to Patel *et al.* [25] can be calculated using the following equation:

$$degradation\ percentage = \left(\frac{C_0 - C_t}{C_0} \right) \times 100\% \qquad (1)$$

with C_0 = initial concentration of RhB (ppm), dan C_t = final concentration of RhB (ppm) at t time.

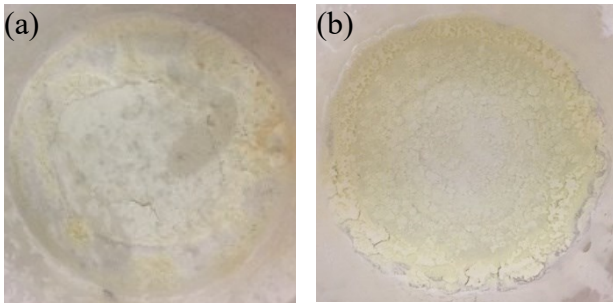

Figure 1. Results after heating for 8 hours with fuel variations (a) urea; and (b) hydrazine.

3. Results and Discussion

3.1 Bismuth oxide synthesis and structure characterisation

In this study, bismuth oxide (Bi_2O_3) was synthesized using SC method with two different fuels. The SC method itself is a synthesis method that involves an exothermic reaction between oxidant and fuel where large amounts of heat energy and gas products, such as CO_2, N_2, and H_2O, will be released. Oxidant generally consists of metal nitrate which acts as a source of metal and oxidizing agents, while a fuel is an organic substance which acts as a reducing agent [26]. In this study, bismuth nitrate pentahydrate ($Bi(NO_3)_3.5H_2O$) acts as oxidant, while urea ($CO(NH_2)_2$) and hydrazine (N_2H_4) act as fuels.

The synthesis of bismuth oxide was initiated with the dilution of bismuth nitrate pentahydrate ($Bi(NO_3)_3.5H_2O$) in a nitric acid solvent. After that, fuel was added then stirred with a speed of 350 rpm to dissolve into the mixture. The solution formed was then heated at 300 ºC for 8 hours. Heating aims to start an exothermic reaction that would occur when the combustion temperature had been reached. The exothermic reaction would produce high energy making it possible to produce the desired product [27].

The synthesized product of bismuth oxide after 8 hours of heating can be seen in Figure 1. In the synthesized product with urea (Figure 1a) shows white with a little yellowish brown color, while the synthesized product using hydrazine (Figure 1b) is white with slight pale

yellow coloring. The resulting powder was then calcined for 4 hours at a temperature of 700 °C.

The bismuth oxide products obtained from both fuels (Figure 2), urea and hydrazine, indicate that bismuth oxide samples formed are in accordance with the claim from Eastaugh *et al.* [28] that bismuth oxide exists as a yellow powder. Bismuth oxide with an energy band gap of 2.3-3.0 eV appears yellow because it absorbs blue and violet lights. The lights blue and violet absorbed will then be emitted as yellow color [29].

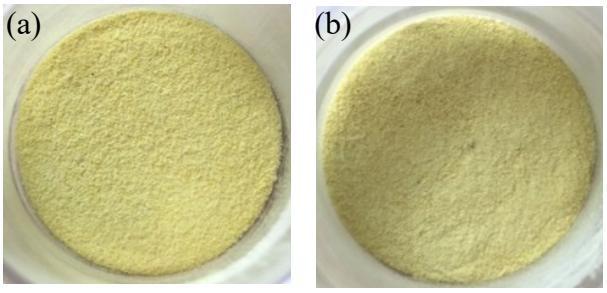

Figure 2. Powder produced from bismuth oxide synthesis with fuel variations (a) urea (BO1); and (b) hydrazine (BO2).

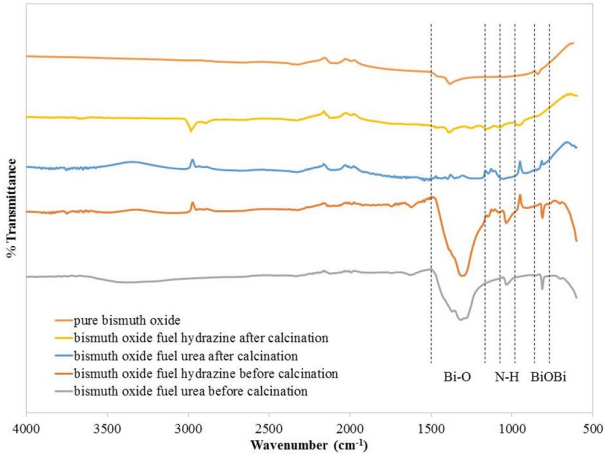

Figure 3. FTIR spectra of pure and synthesized bismuth oxides with fuel variations of urea and hydrazine before and after calcination.

FTIR spectra of both products before and after calcination are presented in Figure 3. FTIR spectra before calcination for Bi_2O_3 fuelled by urea and hydrazine formed successive peaks at wavenumbers 813 and 811 cm^{-1} which indicate the existence of a Bi–O–Bi group [30] and peaks at wavenumber 1300 cm^{-1} which implies Bi–O group. Furthermore, synthesized Bi_2O_3 with urea and hydrazine fuels formed peaks at wavenumbers 1035 and 1034 cm^{-1} which are N–H bending vibrations [31]. Meanwhile, after calcination, FTIR spectra for Bi_2O_3 with urea (BO1) and hydrazine (BO2) generated peaks at wavenumbers 841 and 847 cm^{-1} which indicate the existence of a Bi–O–Bi group [30] and peaks at wavenumbers 1397 and 1377 cm^{-1} which specify the Bi–O

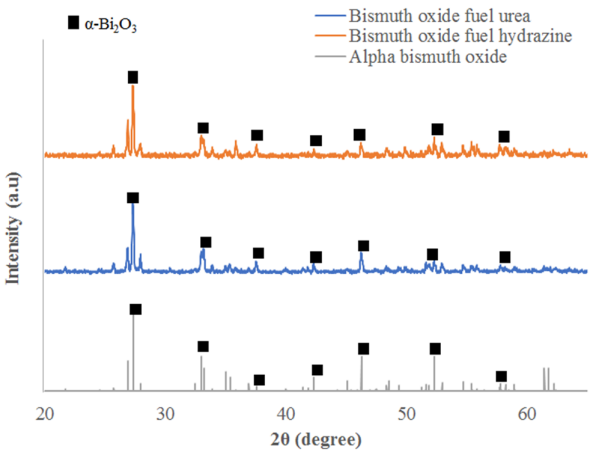

Figure 4. XRD Diffractograms of synthesized bismuth oxide.

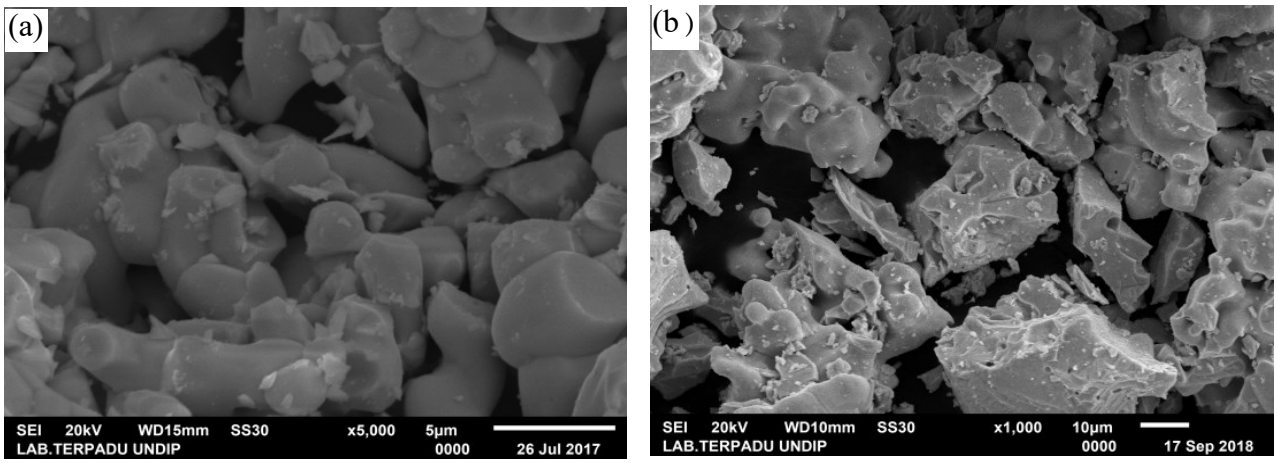

Figure 5. SEM Images of a) BO1; b) BO2.

group [32]. The vibration mode of the two products is the same as the vibration mode of pure bismuth oxide.

The crystalline structure of both BO1 and BO2 products (see Figure 4) possessed the crystal structure of α-Bi_2O_3 (monoclinic) which is indicated by 2θ values of 27.348, 33.213, 46.303 for BO1, and 27.331, 33.043, 46.269 for BO2. These peaks correspond to the α-Bi_2O_3 crystal structure based on the JCPDS database number 41-1449. In calcination at 700 ºC, some bismuth oxide polymorphs, such as: α-Bi_2O_3, β-Bi_2O_3 and γ-Bi_2O_3, can be formed, but alpha bismuth oxide is the most stable compared to other polymorphs, especially when the product is at room temperature [33,34]. This therefore caused the phase α-Bi_2O_3 to be the phase mostly obtained from the synthesis of bismuth oxide.

The SEM images of the two products after calcination are shown in Figure 5. The morphology of BO1 (Figure 5a) with 5000x magnification resembles the shape of corals. Meanwhile, the morphology of the BO2 product (Figure 5b) with a 1000x magnification resembles the shape of boulders. Based on Table 1, BO1 products have an average diameter of particles smaller than BO2 products.

Figure 6 shows the band gap energies of BO1 and BO2, which are 2.73 eV and 2.74 eV, respectively. The results of the study from Iyyapushpam *et al.* [35] claim that α-Bi_2O_3 has a band gap of 2.73 eV. The band gap value is the same as the band gap value for BO1 (Figure 6a) and show little difference from the band gap value for BO2 (Figure 6b). The XRD patterns of BO1 and BO2 also support these results, wherein the resulting bismuth oxide samples have α-Bi_2O_3 crystal structure.

Analysis of surface area using the BET method was used to determine the specific surface area of the urea and hydrazine fueled bismuth oxide samples. Extensive data on the surface of both products are presented in Table 2. Table 2 shows that BO1 surface area is greater than that of BO2. The result is in accordance with the result of SEM analysis which shows that BO1 has a smaller average diameter of particles than BO2.

3.2 Photocatalytic Activity of Bismuth Oxide with Rhodamine B

Bismuth oxide synthesized by the SC method was tested for its photocatalytic activity to degrade RhB dye under exposure of ultraviolet (UV) A light (315-400 nm) in the range of 1 to 4 hours with 1 hour intervals. Absorbance of RhB solution from photocatalysis was measured using UV-Vis spectrophotometry.

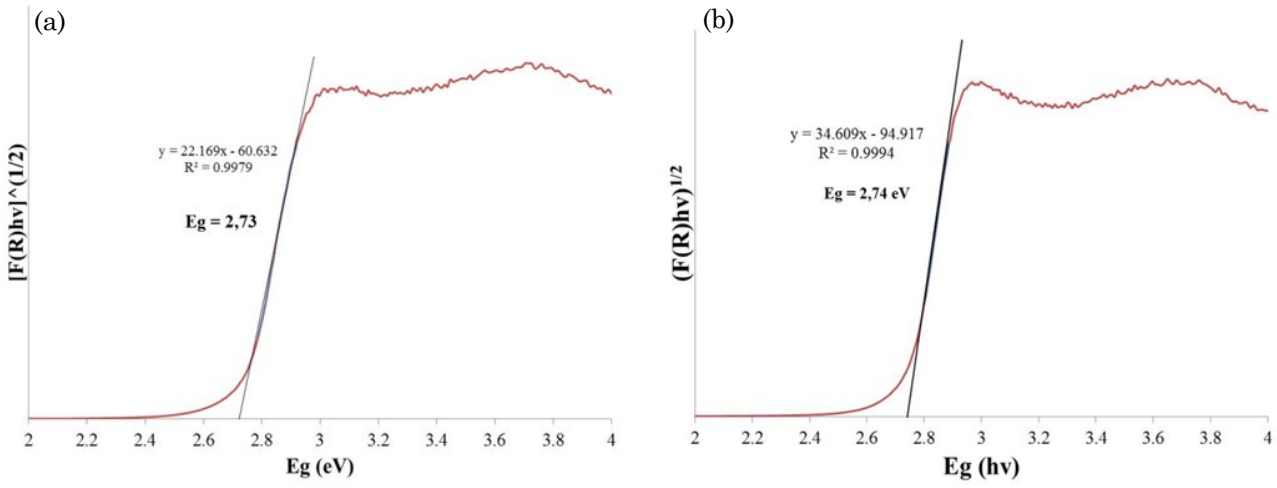

Figure 6. DR-UV Spectra of a) BO1 and b) BO2.

Table 1. The average diameter of BO1 and BO2 products.

Product	Average diameter of particles (μm)
BO1	0.14-10.00
BO2	0.50-37.50

Table 2. The SAA analysis results of BO1 and BO2 products.

Product	Surface Area ($m^2S.g^{-1}$)
BO1	13.180
BO2	9.383

The effect of photocatalytic time on the degradation percentage of RhB concentration by BO1 and BO2 can be seen in Figure 7. Photocatalytic results showed that at 1, 2, 3 and 4 hours BO1 caused greater degradation of RhB compared to BO2. In addition, as a comparison, 2 hours irradiation of RhB without BO1 and BO2 caused no RhB degradation. Meanwhile, the results of the kinetic study shows that the photocatalytic activity of the two products in degrading RhB follows the first order reaction kinetics based on the correlation coefficient (R^2) (see Figure 8) which is in agreement with Wang *et al.* [36] mentioned that degradation of dye molecules by photocatalyst follows first order kinetics, with degradation rate constants of 3.83×10^{-5} s^{-1} and 3.43×10^{-5} s^{-1} for BO1 and BO2 respectively. Therefore, it can be established that BO1 has higher photocatalytic activity than BO2.

The high photocatalytic activity of BO1 product is influenced by several factors such as band gap, crystal structure, surface area and morphology. The DR-UV analysis results obtained (Figure 6) show that the band gap values of the two samples do not show significant difference, which is around 2.7 eV eventhough BO1 shows a little lower band gap energy than BO2. Thus in this case, the comparison of photocatalytic activity for the two products cannot be reviewed by only looking at the band gap value. The photocatalytic activity of bismuth oxide can be seen further by observing the surface area and particle size. Based on the results of the SAA analysis with the BET method shown in Table 2, BO1 products have a larger surface area compared to BO2 products. Large surface area of a material can offer a greater contact area between photocatalysts and pollutants, in this case RhB dye, which is useful for increasing photocatalytic activity on the surface of Bi_2O [37,38].

According to Sood *et al.* [39] the mechanism of photocatalytic degradation by Bi_2O_3 can be understood in the following reaction sequence: when light illuminates the surface of a Bi_2O_3 semiconductor, an electron (e^-) will be excited from the valence band to the conduction band (CB), creating a hole (h^+) in the valence band (VB). A hole in the valence band will react with hydroxyl (OH^-) anion to form hydroxyl radical ($HO\bullet$). The electrons from the conduction band react with O_2 from the atmosphere to form a superoxide radical anion ($O_2\bullet^-$) which then forms $HO_2\bullet$ when it reacts with H^+. Then, $HO_2\bullet$ accepts an electrons to produce HO_2^- which further produces H_2O_2 oxidant when reacted with H^+. The peroxide can decompose into $\bullet OH$ and OH^- which be able to oxidize rhodamine b colors to simpler molecules such as CO_2, H_2O, and others [39].

4. Conclusion

Bismuth oxide synthesis with solution combustion method with the use of urea and hydrazine as fuels shows that characteristics such as band gap and crystal structure are not very much affected by type of fuel used whereas the morphology (crystal size and surface area) is strongly influenced. Effects on morphology result in the difference of products photocatalytic activities in degrading colored substance where the synthesized product with urea (BO1) revealed a higher photocatalytic activity in the degradation of rhodamine B than the synthesized product with hydrazine (BO2).

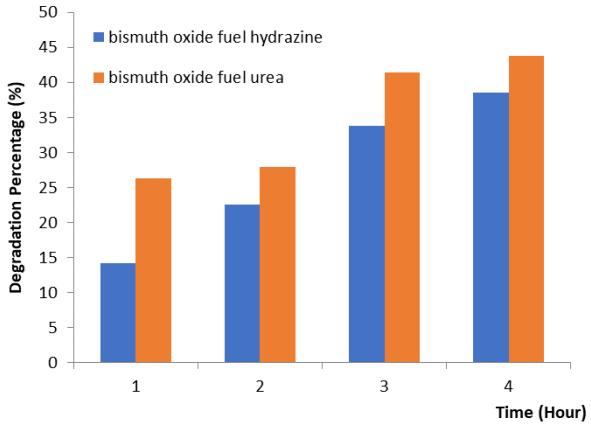

Figure 7. Photocatalytic time effect on the percentage of Rhodamine B concentration degraded by Bi_2O_3 synthesized by urea (BO1) and hydrazine (BO2).

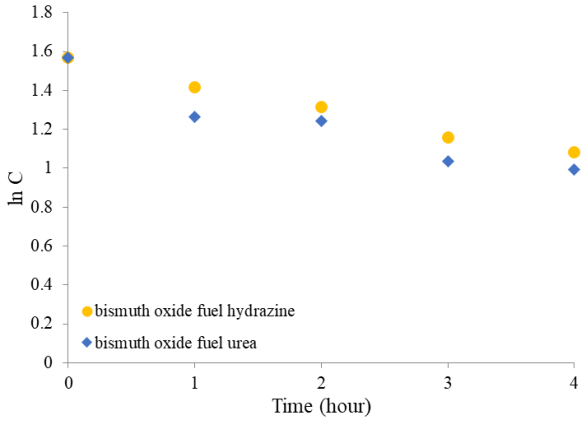

Figure 8. Rhodamin B degradation by BO1 and BO2 follows the first order kinetics.

Acknowledgment

The authors would like to thank the Ministry of Research, Technology and Higher Education, Republic of Indonesia, for financial support through a *Penelitian Hibah Kompetensi (HiKom)* grant, 2018 with the grant no. 101-71/UN7.P4.3/PP/2018. Moreover, first author would like to acknowledge Diponegoro University for financial support during the Postdoctoral/Sabbatical Program, 2017 with the grant no. 990/UN7.P/HK/2017.

References

[1] Xiao, X., Liu, C., Xing, C., Qian, C., Zuo, X., Nan, J., Wang, L. (2013). Facile large-scale synthesis of β-Bi_2O_3 nanospheres as a highly efficient photocatalyst for the degradation of acetaminophen under visible light irradiation. *Applied Catalysis B: Environmental*, 140, 433-443.

[2] Hashimoto, T., Ohta, H., Nasu, H., Ishihara, A., (2016). Preparation and photocatalytic activity of porous Bi_2O_3 polymorphisms. *International Journal of Hydrogen Energy*, 41(18), 7388-7392.

[3] Patil, R.B., Puri, R.K., Puri, V. (2008). Effect of chopping on the properties of bismuth oxide thin films. *Materials Letters*, 62(2), 198-201.

[4] Clapham, P.B. (1967). Preparation and properties of sputtered bismuth oxide films. *British Journal of Applied Physics*, 18(3), 363-366.

[5] Dutta, D.P., Roy, M., Tyagi, A.K. (2012). Dual function of rare earth doped nano Bi_2O_3: white light emission and photocatalytic properties. *Dalton Transactions*, 41(34), 10238-10248.

[6] Joh, D.W., Park, J. H., Kim, D.Y., Yun, B.-H., Lee, K.T. (2016). High performance zirconia-bismuth oxide nanocomposite electrolytes for lower temperature solid oxide fuel cells. *Journal of Power Sources*, 320, 267-273.

[7] Azad, A.M., Larose, S., Akbar, S.A. (1994). Bismuth oxide-based solid electrolytes for fuel cells. *Journal of Materials Science*, 29(16), 4135-4151.

[8] Bhande, S.S., Mane, R.S., Ghule, A.V., Han, S-H. (2011). A bismuth oxide nanoplate-based carbon dioxide gas sensor. *Scripta Materialia*, 65(12), 1081-1084.

[9] Kazakov, S.M., Chaillout, C., Bordet, P., Capponi, J.J., Nunez-Regueiro, M., Rysak, A., Tholence, J.L., Radaelli, P.G., Putilin, S.N., Antipov, E.V. (1997). Discovery of a second family of bismuth-oxide-based superconductors. *Nature*, 390(6656), 148-150.

[10] Kruidhof, H., Seshan, K., van de Velde, G.M.H., de Vries, K.J., Burggraaf, A.J. (1988). Bismuth oxide based ceramics with improved electrical and mechanical properties: Part II. Structural and mechanical properties. *Materials Research Bulletin*, 23(3), 371-377.

[11] Astuti, Y., Arnelli, A., Pardoyo, P., Fauziyah, A., Nurhayati, S., Wulansari, A.D., Andianingrum, R., Widiyandari, H., Bhaduri, G.A. (2017). Studying Impact of Different Precipitating Agents on Crystal Structure, Morphology and Photocatalytic Activity of Bismuth Oxide. *Bulletin of Chemical Reaction Engineering and Catalysis*, 12(3), 478-484.

[12] Ratova, M., Redfern, J., Verran, J., Kelly, P. J. (2018). Highly efficient photocatalytic bismuth oxide coatings and their antimicrobial properties under visible light irradiation. *Applied Catalysis B: Environmental*, 239, 223-232.

[13] Hajra, P., Shyamal, S., Mandal, H., Sariket, D., Maity, A., Kundu, S., Bhattacharya, C. (2019). Synthesis of oxygen deficient bismuth oxide photocatalyst for improved photoelectrochemical applications. *Electrochimica Acta*, 299, 357-365.

[14] Mallahi, M., Shokuhfar, A., Vaezi, M.R., Esmaeilirad, A., Mazinani, V. (2014). Synthesis and characterization of bismuth oxide nanoparticles via sol-gel method. *American Journal of Engineering Research*, 3, 162-165.

[15] Wu, C., Shen, L., Huang, Q., Zhang, Y-C. (2011). Hydrothermal synthesis and characterization of Bi_2O_3 nanowires. *Materials Letters*, 65(7), 1134-1136.

[16] Aruna, S.T., Mukasyan, A.S. (2018). Combustion synthesis and nanomaterials. *Current Opinion in Solid State and Materials Science*, 12(3), 44-50.

[17] Astuti, Y., Fauziyah, A., Nurhayati, S., Wulansari, A.D., Andianingrum, R., Hakim, A.R., Bhaduri, G. (2016). Synthesis of α-Bismuth oxide using solution combustion method and its photocatalytic properties. I*n IOP Conference Series: Materials Science and Engineering,* 107(012006), 1-7.

[18] La, J., Huang, Y., Luo, G., Lai, J., Liu, C., Chu, G. (2013). Synthesis of bismuth oxide nanoparticles by solution combustion method. *Particulate Science and Technology*, 31(3), 287-290.

[19] Sirota, B., Reyes-Cuellar, J., Kohli, P., Wang, L., McCarrol, M.E., Aouadi, S.M. (2012). Bismuth oxide photocatalytic nanostructures produced by magnetron sputtering

deposition. *Thin Solid Films*, 520(19), 6118-6123.

[20] Bohannan, E.W., Jaynes, C.C., Shumsky, M.G., Barton, J.K., Switzer, J.A. (2000). Low-temperature electrodeposition of the high-temperature cubic polymorph of bismuth(III) oxide. *Solid State Ionics*, 131(1), 97-107.

[21] Timmaji, H.K., Chanmanee, W., De Tacconi, N.R., Rajeshwar, K. (2011). Solution combustion synthesis of $BiVO_4$ nanoparticles: effect of combustion precursors on the photocatalytic activity. *Journal of Advanced Oxidation Technologies*, 14(1), 93-105.

[22] Gilabert Albiol, J., Palacios, M. D., Sanz-Solana, V., Mestre, S. (2017). Fuel effect on solution combustion synthesis of $Co(Cr,Al)_2O_4$ pigments. *Boletín de la Sociedad Española de Cerámica y Vidrio*, 56(5), 215-225.

[23] Rasouli, S., Oshani, F., Hashemi, S. (2011). Effect of various fuels on structure and photo-catalytic activity of nanocrystalline TiO_2 prepared by microwave-assisted combustion method. *Progress in Color, Colorants and Coatings*, 4 (2011), 85-94.

[24] Raveendra, R., Prashanth, P., Nagabhushana, B. (2016). Study on the effect of fuels on phase formation and morphology of combustion derived α-Al_2O_3 and NiO nanomaterials. *Advanced Materials Letters*, 7, 216-220.

[25] Patel, V.K., Ganguli, A., Kant, R., Bhattacharya, S. (2015). Micropatterning of nanoenergetic films of Bi_2O_3/Al for pyrotechnics. *RSC Advances*, 5(20), 14967-14973.

[26] Bolaghi, Z.K., Hasheminiasari, M., Masoudpanah, S. (2018). Solution combustion synthesis of ZnO powders using mixture of fuels in closed system. *Ceramics International*, 44(11), 12684-12690.

[27] Canillas, M., Rivero, R., Garcia-Carrodeguas, R., Barba, F., Rodriguez, M.A. (2017). Processing of hydroxyapatite obtained by combustion synthesis. *Boletín de la Sociedad Española de Cerámica y Vidrio*, 56(5), 237-242.

[28] Eastaugh, N., Walsh, V., Chaplin, T., Siddal, R. (2008). *Pigment compendium: a dictionary and optical microscopy of historical pigments*. London, Routledge.

[29] Pimputkar, S., Speck, J.S., DenBaars, S.P., Nakamura, S. (2009). Prospects for LED lighting. *Nature Photonics*, 3(4), 180-182.

[30] Bartonickova, E., Cihlar, J., Castkova, K. (2007). Microwave-assisted synthesis of bismuth oxide. *Processing and Application of Ceramics*, 1(1-2), 29-33.

[31] Diaconeasa, Z., Barbu-Tudoran, L., Coman, C., Leopold, L., Mesaros, A., Pop, O., Rugină, D., Ştefan, R., Tăbăran, F., Tripon, S. (2015). Cerium oxide nanoparticles and its cytotoxicity human lung cancer cells. *Romanian Biotechnological Letters*, 20(4), 10679-10687.

[32] Bandyopadhyay, S., Dutta, A. (2017). Thermal, optical and dielectric properties of phase stabilized δ–Dy-Bi_2O_3 ionic conductors. *Journal of Physics and Chemistry of Solids*, 102, 12-20.

[33] Hong-Yan, D., Wei-Chang, H., Huai-Zhe, X. (2011). A Transition Phase in the Transformation from α-, β- and $\in$- to δ-Bismuth Oxide. *Chinese Physics Letters*, 28(5), 056101 (1-4).

[34] Huang, C., Hu, J., Fan, W., Wu, X., Qiu, X. (2015). Porous cubic bismuth oxide nanospheres: a facile synthesis and their conversion to bismuth during the reduction of nitrobenzenes. *Chemical Engineering Science*, 131, 155-161.

[35] Iyyapushpam, S., Nishanthi, S., Padiyan, D.P. (2013). Photocatalytic degradation of methyl orange using α-Bi_2O_3 prepared without surfactant. *Journal of Alloys and Compounds*, 563, 104-107.

[36] Wang, Q., Hui, J., Yang, L., Huang, H., Cai, Y., Yin, S., Ding, Y. (2014). Enhanced photocatalytic performance of Bi_2O_3/H-ZSM-5 composite for rhodamine B degradation under UV light irradiation. *Applied Surface Science*, 289, 224-229.

[37] Li, H., Sun, B., Xu, Y., Qiao, P., Wu, J., Pan, K., Tian, G., Wang, L., Zhou, W. (2018). Surface defect-mediated efficient electron-hole separation in hierarchical flower-like bismuth molybdate hollow spheres for enhanced visible-light-driven photocatalytic performance. *Journal of colloid and interface science*, 531, 664-671.

[38] Saison, T., Chemin, N., Chanéac, C., Durupthy, O., Ruaux, V., Mariey, L., Maugé, F., Beaunier, P., Jolivet, J-P. (2011). Bi_2O_3, $BiVO_4$, and Bi_2WO_6: impact of surface properties on photocatalytic activity under visible light. *The Journal of Physical Chemistry C*, 115(13), 5657-5666.

[39] Sood, S., Umar, A., Mehta, S. K., Kansal, S. K. (2015). α-Bi_2O_3 nanorods: an efficient sunlight active photocatalyst for degradation of Rhodamine B and 2, 4, 6-trichlorophenol. *Ceramics International*, 41(3), 3355-3364.